# Journal of Materials Chemistry C

Accepted Manuscript

This article can be cited before page numbers have been issued, to do this please use: Y. Luo, Q. Liu, L. Yang, Y. Sun, J. Wang, C. You and B. Sun, *J. Mater. Chem. C*, 2016, DOI: 10.1039/C6TC02796B.

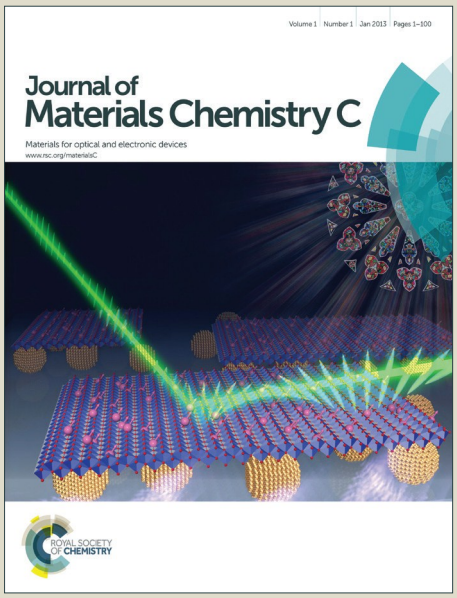




ROYAL SOCIETY OF CHEMISTRY

www.rsc.org/materialsC

View Article Online
DOI: 10.1039/C6TC02796B

Journal Name

ARTICLE

# Magnetic observation of above room-temperature spin transition in vesicular nano-sphere

Received 00th January 20xx,
Accepted 00th January 20xx

DOI: 10.1039/x0xx00000x

www.rsc.org/

Yang-Hui Luo,*[a] Qing-Ling Liu,[a] Li-Jing Yang,[a] Yu Sun,[a, b] Jin-Wen Wang,[a] Chao-Qun You,[a] and Bai-Wang Sun*[a]

Nano-scale materials are acquiring the leading role in the fabrication of new generation devices, especially for practical application of molecular bi-stability. However, the preparation of purely bi-stability nano-objects without surfactant /polymer remains a challenging task. Here, we present a new approach to elaborate spin-crossover (SCO) vesicular nano-sphere with approximately 100nm single-external diameter in $CHCl_3$-$H_2O$ mixture, based on a series SCO complexes ($[Fe(H_2Bpz_2)_2(dialkyl\text{-}bipy)]$) ($H_2Bpz_2$ = dihydrobis(1-pyrazolyl)borate, dialkyl-bipy = $N^4$, $N^{4'}$-dialkyl-(2,2'-bipyridine)-4,4'-dicarbo- xamide, alkyl = propyl, butyl, pentyl, hexyl, heptyl, octyl, nonyl, decyl and cetyl, respectively), through a self-assembly process that is similar to liposomal assembly, with the dialkyl-bipy moiety act as the hydrophobic tail and the $Fe(H_2Bpz_2)$ moiety act as hydrophilic head. This study reveals that the alkyl chain length plays a key role for the formation of these nano-sphere and determination of their spin transition temperatures. The spin transition temperatures for the bulk materials are center around 160 K, and have shown a positive correlation with the alkyl chain length. While for the vesicular nano-sphere in solid state, their transition temperatures have ascended to above room-temperature, and the correlation with the alkyl chain length is nagative. These results have provided an effective strategy for the design of new metal-organic materials for nano-technological applications.

## Introduction

Spin-crossover (SCO) materials are one of the most fascinating class of molecular bi-stability whose spin state can be switched between diamagnetic low-spin (LS) and paramagnetic high-spin (HS) electronic states with the application of various external triggers, such as temperature, pressure, or light.[1, 2] This electronic transition accounts for several changes at the molecular level, affecting the metal-ligand distances (size) and optical properties (UV-vis absorption), in addition to magnetic properties.[3, 4] All of these possibilities have postulated such SCO materials as promising candidates for applications in molecular electronics and spin tronics, communication networks, ultra-high-density memory systems, molecular displays devices, and molecular sensors.[5-7] In terms of practical applications, much effort has been expended to manipulate the SCO materials at the nanoscale: nanoparticles, nanofibers and thin films.[8, 9] Nano-structuration is a fundamental requisite to achieve these application goals.[10] Additionally, the change of the SCO nanoparticles size could dramatically affect their physical properties since electronic bi-stability depends on the collective behaviour of the SCO centres in the material.[11] Consequently, determination of the critical nanoparticle size is therefore an essential aspect of this research. Several notable studies have prepared SCO nanoparticles successfully. In most of the cases, the target compounds were concerned two polymeric iron (II) coordination families: 1D chain Fe(II)-triazole family [12] and 3D [Fe(pyrazine)] $[M(CN)_4]$ (M=Ni, Pd, or Pt) family.[13] Usually, the corresponding SCO nanoparticles were prepared by using micro-emulsions or reverse micelles approach with surfactants[14] or homogeneous approach with functional polymers.[15] These approaches suffer a serious drawback, that is, the presence of excess surfactants or polymers can results to a dilution of the SCO centres in the material, which leads to the weaken of the response when compared with the pure SCO compound, and thus adverse to detection of SCO at nano-meter level.[16] At these points, it should be stressed that the search for new approaches towards new morphologies of SCO nano-objects with wide range of size without surfactant/polymer is of significant importance in the development of molecular bi-stability.

Liposomes, one of the most widely used drug delivery carriers, are spherical vesicles consisting of single or multiple concentric lipid bilayers encapsulating an aqueous compartment.[17] The combination of liposomes with nanoparticles, which enhanced both benefits of specific applications of liposomes and wide functionality of nanoparticles, have been gradually studied over the past years.[18, 19] But the attempts to prepared vesicular nano-sphere that assembly in the way similar to liposome, which may

[a] School of Chemistry and Chemical Engineering, Southeast University, Nanjing, 211189, P.R. China. E-mail: peluoyh@sina.com (Luo); chmsunbw@seu.edu.cn (Sun).
[b] School of Pharmacy, Wannan Medical College, Wuhu, 241002, P.R. China.
Electronic Supplementary Information (ESI) available: [IR spectra of the nine ligands and the nine complexes, crystal structure and refine data of $L_3$, TGA profiles of the ligands $L_6$-$L_{16}$, DLS data of the vesicular nano-sphere and TEM images of the lyophilized samples]. See DOI: 10.1039/x0xx00000x

View Article Online
DOI: 10.1039/C6TC02796B

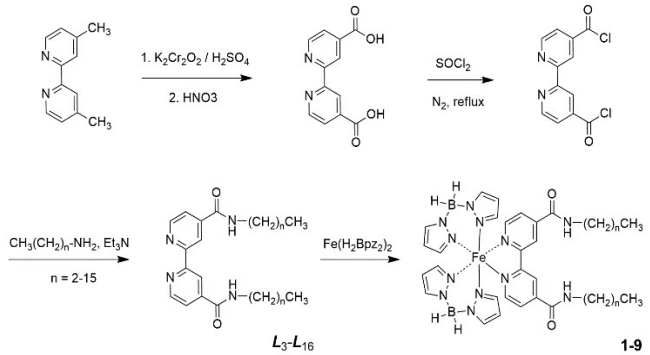


**Scheme 1.** Synthesis procedure for the dialkyl-bipy ligands (***L***$_3$-***L***$_{16}$) and the Fe(II) complexes (**1**-**9**).

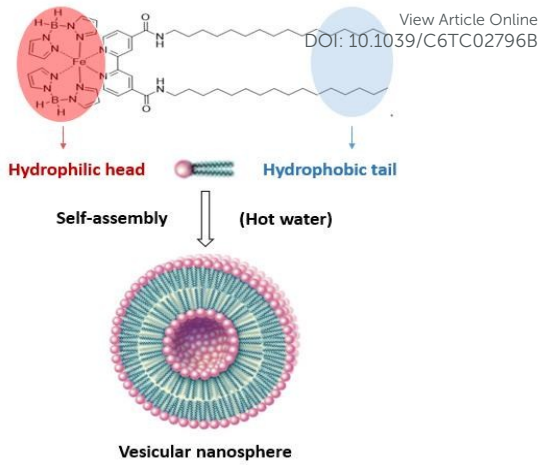


**Scheme 2.** Illustration of the vesicular nano-sphere self-assembly of the Fe(II) complexes.

widely expand the established scope of both liposomes and nanoparticles, still rare, especially in the field of metal-organic nanoparticles. Very recently, Kim[20] and co-authors have reported a series of novel paramagnetic vesicles, which were obtained by self-assembly of ion pairs of iron-containing surfactants in aqueous solution. The magnetization measurements of these vesicles in aqueous solution can act as an effective tool to investigate the critical vesicle concentration, vesicle compositions and distribution of surfactants.

Inspired by the work of Kim, we herein report a new approach to elaborate SCO vesicular nano-sphere based on a series of amphiphilic mononuclear Fe(II) coordination complexes. These complexes are coordinated by two dihydrobis (1-pyrazolyl) borate ($H_2Bpz_2$) ligands and one $N^4$, $N^{4'}$-dialkyl-(2, 2'-bipyridine)-4,4'-dicarboxamide ligand (alkyl = propyl, butyl, pentyl, hexyl, heptyl, octyl, nonyl, decyl and cetyl, the corresponding ligands are denoted as ***L***$_3$, ***L***$_4$, …, ***L***$_{10}$, and ***L***$_{16}$, respectively) (Scheme 1), the corresponding chemical formula of these complexes were assigned to $[Fe(H_2Bpz_2)_2\boldsymbol{L}_3]$ (**1**), $[Fe(H_2Bpz_2)_2\boldsymbol{L}_4]$ (**2**), $[Fe(H_2Bpz_2)_2\boldsymbol{L}_5]$ (**3**), $[Fe(H_2Bpz_2)_2\boldsymbol{L}_6]$ (**4**), $[Fe(H_2Bpz_2)_2\boldsymbol{L}_7]$ (**5**), $[Fe(H_2Bpz_2)_2\boldsymbol{L}_8]$ (**6**), $[Fe(H_2Bpz_2)_2\boldsymbol{L}_9]$ (**7**), $[Fe(H_2Bpz_2)_2\boldsymbol{L}_{10}]$ (**8**) and $[Fe(H_2Bpz_2)_2\boldsymbol{L}_{16}]$ (**9**), respectively (Scheme 1). This kind of complexes have been known as a classical SCO material over 17 years.[21] In our previously work,[22] we have successfully synthesized and characterized a compound $[Fe(H_2Bpz_2)_2(bipy\text{-}NH_2)]\cdot CH_3OH$ (bipy-$NH_2$ = 4, 4'-diamino-2, 2'-bipyridine), and have altered its magnetism from paramagnetic to spin-crossover behaviour. In this work, we attempted to modify the 2, 2'-bpy ligands into amphiphilic molecules. Our ambition is to elaborating vesicular nano-sphere, which will fulfilled by self-assembly of complexes **1**-**9** in a way that similar to liposome assembly, with the alkylated 2, 2'-bpy molecules act as hydrophobic tail and the two $H_2Bpz_2$ molecules act as hydrophilic head (Scheme 2). As we have expected, the measurements of transmission electron microscopy (TEM) and dynamic light scattering (DLS) have provided unambiguous evidence for the formation of vesicular nano-sphere with complexes **4**-**9** in the hot water (60 ℃) (the corresponding nano-sphere are denoted as **NS-4**- **NS-9**), with the single-external diameter increased with the alkyl chain length (from 70 to 100 nm). Note that, complexes **1**-**3** failed to form vesicular nano-sphere, which may ascribed to the fact that the alkyl tails of ligands ***L***$_3$-***L***$_5$ are too short to act as the hydrophobic tail. More importantly, magnetic studies demonstrated that the spin transition temperatures for the bulk materials of complexes **1**-**9** were centre around 160 K, and have shown a positive correlation with the alkyl chain length (which may attribute to the increase of intermolecular contacts with the alkyl chain length). While for the vesicular nano-sphere **NS-4** - **NS-9**, the transition temperatures in the solid state were ascended to above room-temperature (centre around 310 K), and the correlation with the alkyl chain length is negative (which is attribute to the decrease of melting points for the hydrophobic tail with the increasing of alkyl chain length). This increase of spin transition temperatures can be attributed to the enhancement of intermolecular stress caused by vesicular nano-sphere organization.[23]

Although, amphiphilic bipy-based ligands have indeed been used by scientists to fabricate SCO materials into films,[23] liquid crystals,[24] or physical gels,[25] this kind of self-assembly into vesicular nano-sphere with chelating amphiphilic complexes remains un-studied. In addition, a myriad of investigations have been performed to show that the size and geometry of nanoparticles has a big influence on their physical-chemical properties (magnetic, optical or electronic properties),[26] the size of the vesicular nano-sphere in this work are controlled mainly by the alkyl chain length, rather than by concentration suggested by Kim *et. al*.[20] It should be noted that, the nano-sphere in this work is persistent in the solid state after freeze drying, which may open a new door for the practical application of SCO nanoparticles.

## Results and discussion

### Synthesis and characterization

$[Fe(H_2Bpz_2)_2(bipy)]$ related compounds can be classified into the classical tris(diimine) SCO system. On the one hand, this kind of compounds can be synthesized and characterized (by single - crystal X-ray diffraction, IR spectra, element analysis, etc) easily, much modifications concerning on the bipy ligand have been made,[21a, 21b, 21c, 22] and fabrication of this compound into the thin film,[21d] bilayer film or multilayer film [21e] also been performed.

View Article Online
DOI: 10.1039/C6TC02796B

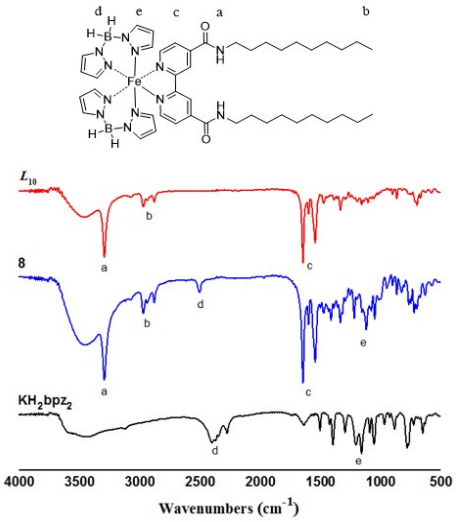


**Figure 1.** IR spectrum of complex **8** and the corresponding starting materials $KH_2Bpz_2$ and $L_{10}$.

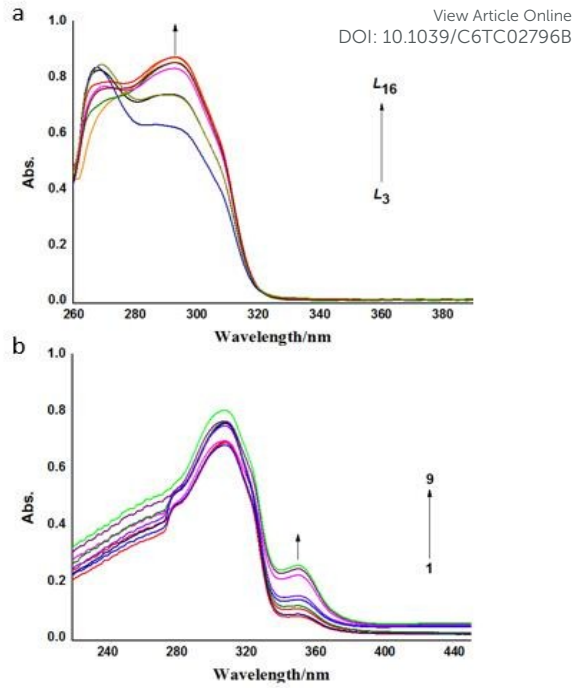


**Figure 2.** UV-vis absorption spectra of the nine $N^4$, $N^{4'}$-dialkyl-(2, 2'-bipyridine)-4, 4'-dicarboxamide) ligands (trace a) and the nine Fe(II) coordination complexes (trace b).

On the other hand, this kind of compounds can display effective switching properties. For complexes **1**-**9,** it is hard to characterize their structures through single - crystal X-ray diffraction due to the long alkyl tails, but their composition can be verified unambiguously by element analysis and IR spectra, as have been approved in our previously work.[22] Ligand $H_2Bpz_2$ was obtained commercially, while ligands $N^4$, $N^{4'}$-dialkyl-(2,2'-bipyridine)-4,4'-dicarboxamide) were synthesized from commercially available compound 4, 4'-dimethyl-(2, 2'-bipyridine) in three steps, including carboxylation, acylation, and condensation of acyl chloride with the corresponding alkyl-amines, respectively (Scheme. 1; details see Supplementary Information).[27] These ligands were obtained as white powders and their structures were confirmed by IR (Figs S1) and $^1$HNMR spectroscopic analyses (Supporting information). In addition, the structure of ligand $L_3$ was investigated by single-crystal X-ray diffraction (Table S1 and Fig S2). To prepare the mononuclear Fe (II) coordination complexes **1**-**9**, we first mixed $KH_2Bpz_2$ (37.2 mg, 0.2 mmol) and $Fe(ClO_4)_2{\cdot}6H_2O$ (36.2 mg, 0.1 mmol) in methanol (10 ml). After stirred the yellow-colour solution for about 20 min at RT under a $N_2$ atmosphere, the white precipitates $KClO_4$ were formed and removed by filtration. The yellow-colour filtrate was then added to a chloroform (20 ml) solution of 0.1 mmol $N^4$, $N^{4'}$-dialkyl-(2,2'-bipyridine)-4,4'-dicarboxamide) ligands at 60 ℃ under a $N_2$ atmosphere, respectively, which resulted a green solution, and followed by the formation of green powders. The resulting suspension were stirred for about 30 mins at 60 ℃, then the green powders of complexes **1**-**9** were collected by filtration at 60 ℃ and washed with methanol (10 ml) and chloroform (10 ml), respectively.[21] After dried vacuum, the yields of these nine complexes were all found to be about 70 %. The composition of these green powders were then analysed by IR spectra (Figs S3), element analysis and mass spectra (supporting information), which were verified the formation of the expected structures.[22] The IR vibrational peak assignments in the case of complex **8** (Fig. 1) revealed that this kind of complexation have shown slight influence on the vibrational peak of ligand $L_{10}$ (peaks a, b, c), but a dramatically red-shift of peak d (from 2397 to 2495 $cm^{-1}$) and blue-shift of peak e (from 1150 to 1103 $cm^{-1}$) for $KH_2Bpz_2$, which can be ascribed to the distortion of $H_2Bpz_2^-$ after complexation. The IR spectra of the other eight complexes (**1**-**7** and **9**) all have shown similar trends as **8**.

### UV-vis absorption

We first investigated the UV-vis absorption spectra of the nine $N^4$,$N^{4'}$-dialkyl-(2,2'-bipyridine)-4,4'-dicarboxamide) ligands, their exhibit two absorption bands at 269 and 290 nm (Fig. 2a), which can be assigned to the n···π* and π···π* transition between the ligands, respectively.[28] For ligands $L_3$-$L_5$, the n···π* transition have shown stronger intensity than π···π* transition. While for ligands $L_6$-$L_{16}$, the condition is reverse, the longer the alkyl tails, the stronger intensity of π···π* transition, demonstrating a striking influence of alkyl tails on the absorption properties, which will certainly affect the ligand field of these ligands. Complexation of these ligands with $Fe(H_2Bpz_2)_2$ resulted 25 nm red-shift of n···π* transition, as well as 43 nm red-shift of π···π* transition, accompanied by decrease in intensity. This red-shift is indicative of the successful preparation of these nine Fe (II) coordination complexes.

### Vesicular nano-sphere

To prepare the vesicular nano-sphere,[29] 20 mg of the above synthesized Fe (II) coordination complexes were added to chloroform (60 ml) solution, in a 250 ml flask, the resulting suspension was then ultrasonic under 60 ℃ for about 10 mins, giving a clear solution. After that, the chloroform solution was evaporated slowly with a rotary evaporator under vacuum at

View Article Online
DOI: 10.1039/C6TC02796B

Journal Name

ARTICLE

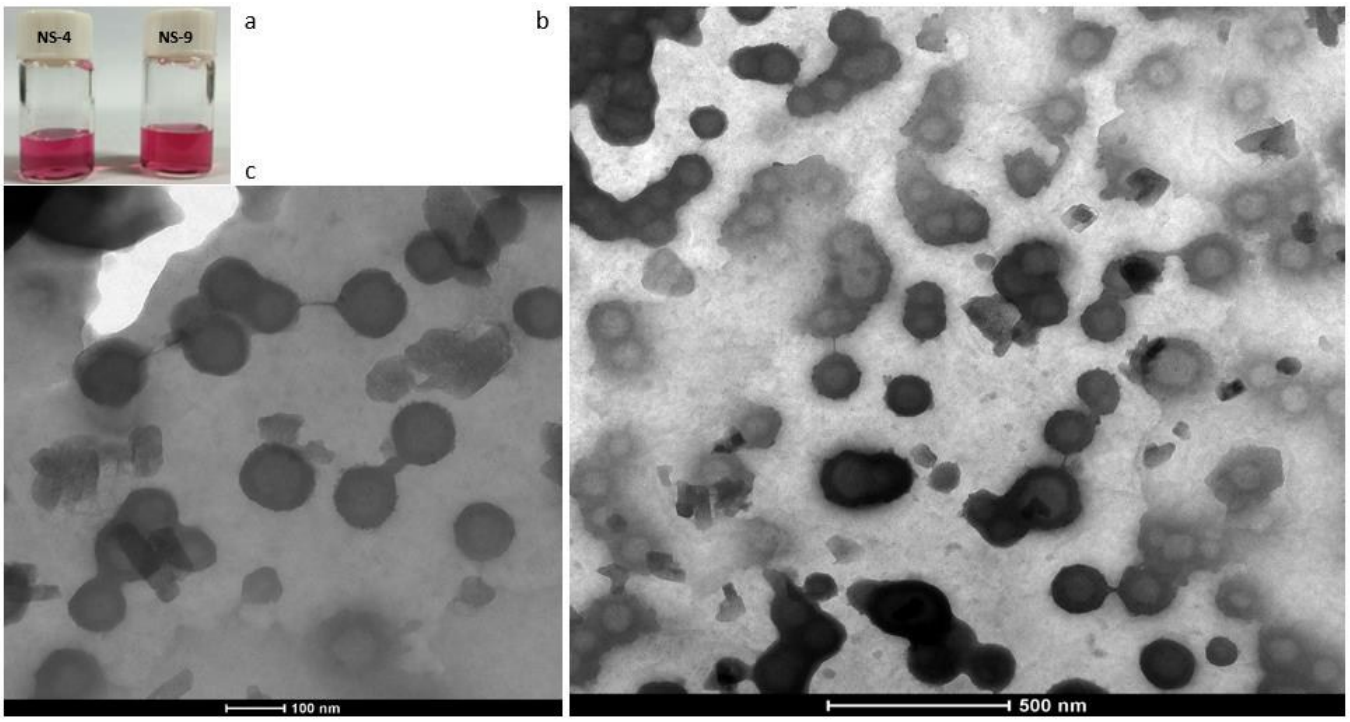


**Figure 3.** The character of vesicular nano-sphere. **a**, Nano-sphere **NS-4** - **NS-9** all exhibit purple-red colour in water, the **NS-4** and **NS-9** were selected for comparison. **b**, TEM image (Tecnai-G$^2$ 20 E-TWIN 200 kV) of **NS-9** at 500 nm scale. **c**, TEM image of **NS-9** at 100 nm scale, the cavity (the grey-white region on the nano-sphere) and periphery of the nano-sphere have been highlighted.

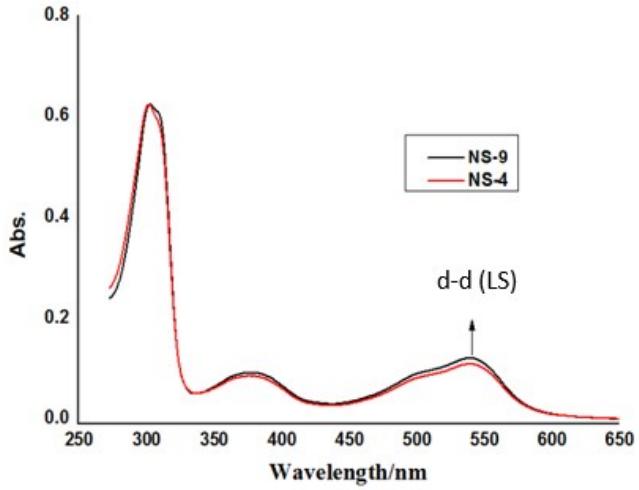


**Figure 4.** UV-vis absorption spectra of **NS-4** and **NA-9** in water, the others (**NS-5-8)** are shown identical spectra with them.

60 ℃, giving a homo-disperse dry film of the Fe (II) complexes. Soon after, 20 ml hot water (60 ℃) was added into the in-prepared film, and the flask was shake vigorously under constant temperature for about 30 mins, a stable purple-red species was obtained (Fig. 3a). Note that, for complexes **1**-**3**, their films in hot water formed suspensions, and the suspensions were precipitated upon cooling to room-temperature, demonstrating the failure of vesicular nano-sphere self-assembly. This failure may be interpreted by the fact that the alkyl tails in ligands $L_3$-$L_5$ are too short to act as hydrophobic tail for the liposomal assembly. While for complexes **4**-**9**, their purple-red suspensions were stable to room-temperature, indicating the stable existence of vesicular nano-sphere (denoted as **NS-4** - **NS-9**).

We first investigated the absorption properties of these vesicular nano-sphere, they were shown almost identical spectra (Fig. 4). Compared with the bulk materials, the π···π* transition of the dialkyl-bipy moiety in vesicular nano-sphere underwent a 32 nm red shift to 365 nm. In addition, a new broad band at around 550 nm has been generated, which can be assigned to the d-d transition of LS state Fe(II) ions.[28] This d-d transition band indicate the LS state of these vesicular nano-sphere at around room-temperature, which was in accordance

View Article Online
DOI: 10.1039/C6TC02796B



with the purple-red colour of the solution (Fig. 3a) and was verified by the magnetic measurements (see below). These results can be ascribed to the increase of intermolecular stress which derived from vesicular nano-sphere organization.

The morphology of these vesicular nano-sphere were investigated by transmission electron microscopy (TEM, Figure 3) and dynamic light scattering (DLS, Figure S4 and Table S2) measurements. Before these measurements, these purple-red species were purified by milli-pore filter (Φ50 (0.2/0.45μ)). Shown in Fig. 3b and 3c were the TEM images of **NS-9** at 500 and 100 nm scale, respectively. They are clearly shown the formation of substantially uniformed nano-sphere with large cavity, the cavity was represented by the grey-white region on the nano-sphere. The other nano-sphere (**NS-4**-**NS-8**) also shown similar images as **NS-9** except smaller in size. These images provided direct evidences for the formation of vesicular nano-sphere through liposomal self-assembly. On the one hand, the longer alkyl tails resulted to larger diameter distribution of nano-sphere. The single-external diameter of **NS-4** was distributed at around 70 nm, while for **NS-7**, this value was increased to 100 nm (Figure S4 and Table S2). One the other hand, **NS-8** and **NS-9** have shown almost identical diameter distribution with **NS-7**, which indicated that the 100 nm or more single-external diameter distribution may be the maximal size for stable existence of this kind of nano-sphere in water. Compared with the vesicles that self-assembled by iron-containing surfactants have shown various sizes changing from 100 to 200 nm,[20] the vesicular nano-sphere in this work, which were self-assembled by chelating amphiphilic complexes, may compressed more closely to give a sub-100 nm size.

**Magnetic properties**

To explore the influence of vesicular nano-sphere self-assembly on the spin state of the Fe (II) complexes, temperature-dependent magnetic measurements in temperature range 400-200 K for the six lyophilized vesicular nano-sphere (**NS-4** – **NS-9**) were performed, the results were compared with the corresponding bulk materials (temperature range 305-100K). Shown in Fig. 5 were the χm T versus T plots of them. For the bulk materials **1**-**9**, the χm T values are all about 3.3 $cm^3mol^{-1}K$ at the upper temperature limit, typical value for a HS Fe(II) atom. Upon cooling to below 200 K, the nine complexes were all underwent one-step complete SCO transition abruptly, with the spin transition temperatures for **1**-**9** in the range of 154-178 K. Moreover, the transition temperatures have shown a positive correlation with the length of the alkyl tails, that is: the longer the alkyl tails, the higher the transition temperatures. These results may attribute to the increase of intermolecular contacts with the alkyl chain length. While for the six lyophilized vesicular nano-sphere, the χm T values were about 2.9 $cm^3mol^{-1}K$ at 400 K, indicating a complete HS state. Upon cooling, the χm T values of **NS-4** begin to decrease below 353 K, and gradually reach to complete LS state at about 260 K, giving a gradual spin-transition with transition temperature of 332 K. While for **NS-5**-**NS-9**, the χm T values begin to decrease below 350, 346, 342, 336 and 327 K, respectively, and all gradually reach to complete

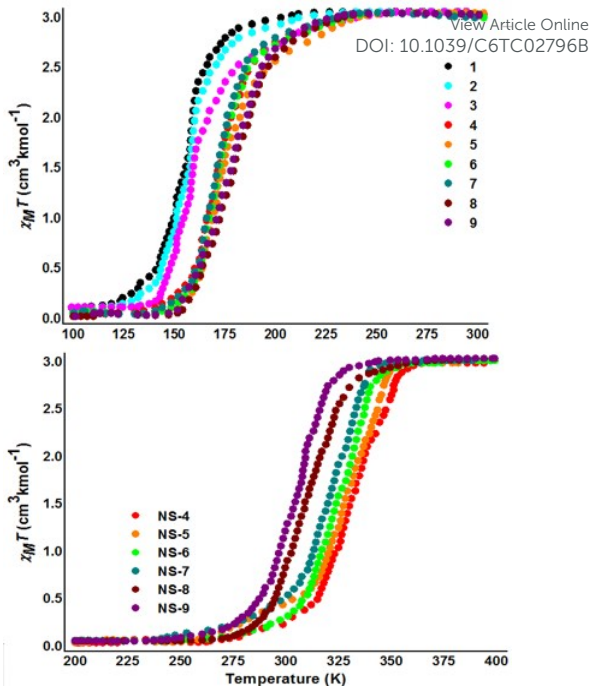


**Figure 5.** Temperature dependence of χm T versus T plots of the bulk materials (**1**-**9**) in temperature range 305-100 K and lyophilized vesicular nano-sphere (**NS-4** – **NS-9**) in temperature range 400-200 K, with an applied magnetic field of 2000 Oe.

LS state at about 260 K with transition temperatures of 329, 324, 321, 310 and 305 K, respectively.

It is Interesting that the spin transition temperatures of these vesicular nano-sphere have shown a negative correlation with the alkyl chain length, that is: the longer the alkyl tails, the lower the transition temperatures, which is in contrary to the bulk materials. These phenomenon can be interpreted as follows: At around room-temperature, the nano-sphere organization compress the Fe(II) complex into LS state; While at higher temperature, the vesicular nano-sphere release the stress imposed by the organization, which thus induce to HS state; In particular, the complete HS state should be obtain when the alkyl tails melt; When the temperature is above the melting point (at about 400 K), the properties of the vesicular nano-sphere are similar to those of the complex in the bulk; Thereby, upon cooling from 400 K, the χm T values of the vesicular nano-sphere begin to decrease at around the melting point of alkyl tails. The thermal analysis (TGA/DSC) of ligands $\boldsymbol{L}_6$-$\boldsymbol{L}_{16}$ were shown in Figure S5, which shown that the melting points the six ligands were found to be 347, 345, 344, 342, 339 and 336 K, respectively. The negative correlation between the spin transition temperatures and the alkyl chain length can then be understood.

After the above magnetic measurements, the six purple-red lyophilized species were further dispersed in hot water (60 ℃), which resulted a purple-red suspensions that was almost identical with the un-lyophilized samples. TEM measurements of the re-obtained suspensions (Figure S6) indicate the persistence of this vesicular nano-sphere in the solid state, even over a large temperature range (below 400 K).

View Article Online
DOI: 10.1039/C6TC02706B



## Experimental

### Materials and methods

All syntheses were performed under ambient conditions. $Fe(ClO_4)_2{\cdot}6H_2O$, $KH_2Bpz_2$, the nine alkyl-amines (propylamine, butylamine, pentylamine, hexylamine, heptylamine, octylamine, nonylamine, decylamine and cetylamine), $SOCl_2$, 4, 4'-dimethyl-(2, 2'-bipyridine), $K_2Cr_2O_2$, $H_2SO_4$ and $HNO_3$ were all obtained commercially and used as received. Elemental analyses were performed by a Vario-EL III elemental analyser for carbon, hydrogen, and nitrogen. Infrared spectra were recorded on a SHIMADZU IR prestige-21 FTIR-8400S spectrometer in the spectral range 4000-500 $cm^{-1}$, with the samples in the form of potassium bromide pellets. UV-vis absorption spectra were recorded with a Shimadzu UV-3150 double-beam spectrophotometer. $^1H$ NMR spectra were obtained using a DPX 500 MHz spectrometer (Bruker Daltonics Inc., USA). MS was performed using a xevo g2 qtof instrument (Waters Co. Ltd. USA). TEM images of the vesicular nano-sphere were recorded on a Tecnai-$G^2$ 20 E-TWIN 200 KV TEM. The freeze drying of the liposomal assembly nanoparticles were conducted on a Labconco FreeZone 6L lyophilizer. DLS characterization was performed on a Zetasizer 3000HS dynamic light scattering instrument (Malvern instruments Ltd., UK). Thermal analysis were performed using a Mettler-Toledo TGA/DSC STARe System at a heating rate of 10 K $min^{-1}$ under an atmosphere of dry $N_2$ flowing at 20 $cm^3min^{-1}$. Temperature-dependent magnetization (M-T) of these coordination Fe (II) complexes (**1**-**9**) as well as the vesicular nano-sphere (**NS-4** - **NS-9**) were measured in the temperature range 305-5 and 400-200 K, respectively, by using a quantum design vibrating sample magnetometer in a physical property measurement system (PPMS). Measurements were performed on freshly prepared powders and lyophilized nano-sphere of 10-15 mg.

### Synthetic procedures

Compound 4, 4' -dicarboxy-2, 2'-bipyridine was prepared according to the literate[30] (Scheme 1): 1.0 g (5.43 mmol) 4,4'-dimethyl-2,2'-bipyridine was added to a 35 ml solution of sulfuric acid (98%), then 6.34 g (21.56 mmol) potassium dichromate were added into the resulting solution within 30 mins, with temperature between 70 and 80 ℃. After stirred for about 2 h, the deep green reaction mixture was poured in 200 ml of ice water and a light yellow solid was formed immediately. The solid was filtered and washed with water. The obtained light yellow solid was then further purified by refluxing in 35 ml 65% nitric acid for 6 h. Then to this solution, ice were poured and the temperature was cooled to about 5 ℃. The products of compound 4, 4' -dicarboxy-2, 2'-bipyridine was precipitated as white solid, then filtered, washed with water and dried vacuum.

Compound 4, 4' -dichlorocarbonyl-2, 2'-bipyridine was prepared by refluxing a suspension of 2 mmol compound 4, 4' -dicarboxy - 2, 2'-bipyridine in dry thionyl chloride (20 ml) under N2 atmosphere overnight. The excess thionyl chloride was removed under vacuum leaving a yellow solid which was used immediately and without purification for the next step.[31]

The ligands were prepared by condensation of compound 4, 4' -dichlorocarbonyl-2, 2'-bipyridine with two equivalents of alkyl-amines (propylamine, butylamine, pentylamine, hexylamine, heptylamine, octylamine, nonylamine, decylamine and cetylamine)[31]. To a stirred solution of 4, 4' -dichlorocarbonyl-2, 2'-bipyridine (1 mmol) in dry $CH_2Cl_2$ (10 ml), 2 mmol alkyl-amines and 3 mmol trimethylamine in 10 ml dry $CH_2Cl_2$ solution was added dropwise, over two minutes. The resulting solution was stirred for 4 h and the white precipitate was filtered and washed with 20 ml $CH_2Cl_2$ and 20 ml $Et_2O$, affording the corresponding products (***L*₃**-***L*₁₀** and ***L*₁₆**) as white solid in more than 80 % yield. The structures of these nine ligands were investigated by IR (Figure S1) and $^1H$-NMR spectra. ***L*₃** ($C_{18}N_4H_{22}O_2$), IR (KBr pellet, $cm^{-1}$): 3288, 2966, 2874, 1638, 1593, 1541, 1467, 1329, 1153, 1099, 861, 692, 664. $^1H$-NMR $\delta$(ppm): 8.88(d, 1H), 8.67(s, 1H), 8.02(m, 1H), 7.38(d, 1H), 3.18(m, 2H), 1.60(m, 2H), 0.90(m, 3H). ***L*₄** ($C_{20}N_4H_{26}O_2$), IR (KBr pellet, $cm^{-1}$): 3294, 2958, 2874, 1638, 1593, 1541, 1466, 1328, 1156, 1098, 865, 692, 667. $^1H$-NMR $\delta$(ppm): 8.88(d, 1H), 8.67(s, 1H), 8.03(m, 1H), 7.38(d, 1H), 3.06(m, 2H), 1.52(m, 2H), 1.31(m, 3H), 0.90 (m, 3H). ***L*₅** ($C_{22}N_4H_{30}O_2$), IR (KBr pellet, $cm^{-1}$): 3293, 2960, 2875, 1638, 1593, 1541, 1467, 1329, 1155, 1099, 868, 699, 679. $^1H$-NMR $\delta$(ppm): 8.88(d, 1H), 8.66(s, 1H), 8.03(m, 1H), 7.38(d, 1H), 3.06(m, 2H), 1.52(m, 2H), 1.29-1.31(m, 4H) 0.90(m, 3H). ***L*₆** ($C_{24}N_4H_{34}O_2$), IR (KBr pellet, $cm^{-1}$): 3294, 2970, 2873, 1638, 1593, 1541, 1467, 1335, 1158, 1099, 866, 692, 665. $^1H$-NMR $\delta$(ppm): 8.88(d, 1H), 8.66(s, 1H), 8.03(m, 1H), 7.38(d, 1H), 3.06(m, 2H), 1.52(m, 2H), 1.29-1.31(m, 6H) 0.88(m, 3H). ***L*₇** ($C_{26}N_4H_{38}O_2$), IR (KBr pellet, $cm^{-1}$): 3290, 2967, 2875, 1638, 1593, 1541, 1467, 1334, 1156, 1092, 861, 693, 664. $^1H$-NMR $\delta$(ppm): 8.88(d, 1H), 8.66(s, 1H), 8.03(m, 1H), 7.38(d, 1H), 3.06(m, 2H), 1.52(m, 2H), 1.29-1.31(m, 8H) 0.88(m, 3H). ***L*₈** ($C_{28}N_4H_{42}O_2$), IR (KBr pellet, $cm^{-1}$): 3289, 2967, 2877, 1638, 1593, 1541, 1467, 1335, 1157, 1099, 864, 692, 680. $^1H$-NMR $\delta$(ppm): 8.88(d, 1H), 8.66(s, 1H), 8.03(m, 1H), 7.38(d, 1H), 3.06(m, 2H), 1.52(m, 2H), 1.29-1.31(m, 10H) 0.88(m, 3H). ***L*₉** ($C_{30}N_4H_{46}O_2$), IR (KBr pellet, $cm^{-1}$): 3292, 2968, 2876, 1638, 1593, 1541, 1467, 1334, 1158, 1099, 865, 692, 664. $^1H$-NMR $\delta$(ppm): 8.88(d, 1H), 8.67(s, 1H), 8.03(m, 1H), 7.38(d, 1H), 3.06(m, 2H), 1.52(m, 2H), 1.29-1.31(m, 12H) 0.88(m, 3H). ***L*₁₀** ($C_{32}N_4H_{50}O_2$), IR (KBr pellet, $cm^{-1}$): 3309, 3066, 2954, 2922, 2852, 1633, 1590, 1531, 1494, 1473, 1383, 1296, 1170, 1129, 1038, 1014, 1058, 854, 780, 695. $^1H$-NMR $\delta$(ppm): 8.87(d, 1H), 8.67(s, 1H), 8.02(m, 1H), 7.37(d, 1H), 3.04(m, 2H), 1.52(m, 2H), 1.27-1.29(m, 14H), 0.88(m, 3H). ***L*₁₆** ($C_{44}N_4H_{74}O_2$), IR (KBr pellet, $cm^{-1}$): 3448, 2920, 2850, 2677, 2491, 1638, 1529, 1474, 1398, 1384, 1366, 1296, 1186, 1125, 1036, 1013, 766, 683, 570, 504. $^1H$-NMR $\delta$(ppm): 8.87(d, 1H), 8.67(s, 1H), 8.01(m, 1H), 7.37(d, 1H), 3.05(m, 2H), 1.53(m, 2H), 1.26-1.28(m, 26H), 0.87(m, 3H).

Complexes **1**-**9** were prepared according to our previously work[22] as well as literature[32]: To a 10 mL methanol solution with 4 mmol $KH_2Bpz_2$, 5 mL methanol solution with 2 mmol $Fe(ClO_4)_2{\cdot}6H_2O$ was added under a $N_2$ atmosphere. The mixture was stirred for 10 min before decanted off and filtered. The precipitate of potassium perchlorate was washed with 5 mL of methanol. The methanol solution containing $Fe(H_2Bpz_2)_2$ were collected, and it was then added dropwise into a 20 mL $CHCl_3$ solutions with 1 mmol the above synthesized ligands at

temperature of 60℃ under a $N_2$ atmosphere, green powders was formed immediately. After stirred for about 30 mins, the green powders were filtrated under 60℃, and washed with 10 ml methanol and 10 ml $CHCl_3$, respectively. The composition of the coordination complexes (**1**-**9**) were investigated by element analysis, IR (Figure S3) and mass spectra. **1** $[Fe(H_2Bpz_2)_2\boldsymbol{L}_3]$ $(FeC_{30}N_{12}H_{38}B_2O_2)$ , anal. calcd. (%): C, 53.23; N, 24.85; H, 5.66. Found: C, 53.38; N, 25.12; H, 5.36. IR (KBr pellet, $cm^{-1}$): 3348, 3288, 2918, 2854, 2395, 1638, 1593, 1538, 1484, 1431, 1230, 1145, 1111, 1042, 831, 775, 690, 655, 548, 490; *m/z* = 676.28 (100.0%), 675.28 (42.0%), 677.28 (30.3%); **2** $[Fe(H_2Bpz_2)_2\boldsymbol{L}_4]$ $(FeC_{32}N_{12}H_{42}B_2O_2)$ , anal. calcd. (%): C, 54.52; N, 23.86; H, 6.01. Found: C, 53.86; N, 23.42; H, 5.89. IR (KBr pellet, $cm^{-1}$): 3345, 3288, 2917, 2854, 2394, 1640, 1592, 1538, 1489, 1438, 1238, 1156, 1122, 1047, 835, 766, 698, 662, 553, 499; *m/z* = 704.31 (100.0%), 703.31 (48.6%), 705.31 (41.0%); **3** $[Fe(H_2Bpz_2)_2\boldsymbol{L}_5]$ $(FeC_{34}N_{12}H_{46}B_2O_2)$ , anal. calcd. (%): C, 55.71; N, 22.95; H, 6.33. Found: C, 55.26; N, 22.49; H, 6.19. IR (KBr pellet, $cm^{-1}$): 3347, 3290, 2919, 2855, 2394, 1639, 1595, 1539, 1488, 1433, 1238, 1146, 1112, 1039 837, 785, 709, 665, 548, 512; *m/z* = 732.34 (100.0%), 731.34 (48.6%), 733.34 (43.2%); **4** $[Fe(H_2Bpz_2)_2\boldsymbol{L}_6]$ $(FeC_{36}N_{12}H_{50}B_2O_2)$ , anal. calcd. (%): C, 56.81; N, 22.09; H, 6.63. Found: C, 56.44; N, 21.67; H, 6.22. IR (KBr pellet, $cm^{-1}$): 3340, 3280, 2912, 2850, 2390, 1637, 1599, 1539, 1485, 1433, 1229, 1140, 1121, 1038, 834, 777, 692, 656, 552, 501; *m/z* = 760.37 (100.0%), 759.38 (53.9%), 761.37 (44.9%); **5** $[Fe(H_2Bpz_2)_2\boldsymbol{L}_7]$ $(FeC_{38}N_{12}H_{54}B_2O_2)$ , anal. calcd. (%): C, 57.84; N, 21.31; H, 6.90. Found: C, 57.38; N, 20.87; H, 6.63. IR (KBr pellet, $cm^{-1}$): 3344, 3287, 2919, 2855, 2392, 1648, 1593, 1539, 1488, 1421, 1233, 1146, 1118, 1042, 833, 773, 691, 651, 540, 495; *m/z* = 788.40 (100.0%), 787.41 (54.2%), 789.41 (46.5%); **6** $[Fe(H_2Bpz_2)_2\boldsymbol{L}_8]$ $(FeC_{40}N_{12}H_{58}B_2O_2)$ , anal. calcd. (%): C, 58.79; N, 20.58; H, 7.16. Found: C, 58.33; N, 19.95; H, 6.88. IR (KBr pellet, $cm^{-1}$): 3345, 3287, 2919, 2855, 2398, 1638, 1593, 1538, 1482, 1433, 1235, 1135, 1116, 1048, 832, 779, 694, 665, 544, 493; *m/z* = 816.43 (100.0%), 815.44 (54.7%), 817.44 (49.4%); **7** $[Fe(H_2Bpz_2)_2\boldsymbol{L}_9]$ $(FeC_{42}N_{12}H_{62}B_2O_2)$ , anal. calcd. (%): C, 59.68; N, 19.89; H, 7.40. Found: C, 59.35; N, 19.38; H, 7.13. IR (KBr pellet, $cm^{-1}$): 3348, 3288, 2924, 2845, 2412, 1638, 1591, 1542, 1476, 1434, 1220, 1145, 1118, 1042, 833, 777, 693, 651, 538, 499; *m/z* = 844.47 (100.0%), 843.47 (42.3%), 845.47 (40.0%); **8** $[Fe(H_2Bpz_2)_2\boldsymbol{L}_{10}]$ $(FeC_{44}N_{12}H_{66}B_2O_2)$, anal. calcd. (%): C, 60.51; N, 19.26; H, 7.62. Found: C, 60.14; N, 18.95; H, 7.13. IR (KBr pellet, $cm^{-1}$): 3444, 3304, 2918, 2870, 2395, 1638, 1618, 1545, 1377, 1278, 1108, 1087, 1068, 988, 856, 786, 694, 645, 530, 488; *m/z* = 872.50 (100.0%), 871.50 (42.0%), 873.50 (41.4%); **9** $[Fe(H_2Bpz_2)_2\boldsymbol{L}_{16}]$ $(FeC_{56}N_{12}H_{90}B_2O_2)$, anal. calcd. (%): C, 64.57; N, 16.15; H, 8.72. Found: C, 64.18; N, 15.89; H, 8.15. IR (KBr pellet, $cm^{-1}$): 3314, 3221, 2920, 2850, 2739, 2678, 2492, 2218, 1633, 1592, 1528, 1474, 1401, 1195, 1122, 1038, 779, 696, 651, 549, 498; *m/z* = 1040.68 (100.0%), 1041.69 (73.2%), 1039.69 (54.3%), 1040.69 (34.4%).

**Single Crystal X-Ray Crystallography**

The single-crystal X-ray diffraction data of ligand $\boldsymbol{L}_3$ was collected with graphite-monochromated Mo Ka radiation (λ = 0.071073 nm). A Rigaku SCXmini diffractometer with the v-scan technique was used[33]. The lattice parameters were integrated using vector analysis and refined from the diffraction matrix, the absorption correction was carried out by using Bruker SADABS program with the multi-scan method. The structures were solved by full-matrix least-squares methods on all F2 data. The
SHELXS-97 and SHELXL-97 programs[34] were used for structure solution and structure refinement, respectively. The molecular graphics were prepared by using the mercury program[35]. A summary of pertinent information relating to unit cell parameters are provided in Table S1. The crystal structure and packing motif of ligand L3 were shown in Figure S2.

## Conclusions

In summary, we have demonstrated that a series of vesicular nano-sphere, which have been obtained through similar-liposomal self-assembly, can exist stably in water with specific size. Hydrophilic alkyl tails play a dominant role in driving the self-assembly process, determining the final size and spin transition properties of the vesicular nano-sphere. To the best of our knowledge, this is the first magnetic observation of above room-temperature spin transition in vesicular nano-sphere. The increase of spin-transition temperature via nano-sphere organization suggest that the present strategy may open new door for the construction of self-assembled nanoparticles for other application-oriented purposes. Further application of this vesicular nano-sphere self-assembly strategy in other functional metal-organic materials are thus ongoing in our laboratories.

## Acknowledgements

This research was based on work supported by the Natural Science Foundation of China (Grant No. 21371031), International S&T Cooperation Program of China (No. 2015DFG42240) and PAPD of Jiangsu Higher Education Institutions. Y.H. Luo thanks the Scientific Research Foundation of Graduate School of Southeast University (No. YBPY1409) for financial support.

## Notes and references

1 (a)Bousseksou, G. Molnar, L. Salmon, W. Nicolazzi, *Chem Soc Rev* 2011, **40**, 3313; (b) Spin-Crossover Materials, Properties and Applications (Ed.: M. A. Halcrow), Wiley, Hoboken, 2013.
2 (a)H.-J. Krüger, *Coordin Chem Rev*, 2009, **253**, 2450; (b) P. Gütlich, H. A. Goodwin,*Top. Curr. Chem* 2004, **233**, 1; (c) J.-F. Letard, P. Guionneau, L. Goux-Capes, *Top. Curr. Chem*, 2004, **235**, 221.
3 (a) M. A. Halcrow, *Chem Soc Rev*, 2011, **40**, 4119; (b) I. B. Bersuker, *Chem Rev*, 2013, **113**, 1351.
4 (a) O. Kahn, *Science*, 1998, **279**, 44; (b) K. P. Kepp, *Coordin Chem Rev* 2013, **257**, 196;
5 A. Rotaru, J. Dugay, R. P. Tan, I. A. Guralskiy, L. Salmon, P. Demont, J. Carrey, G. Molnar, M. Respaud, A. Bousseksou, *Adv Mater*, 2013, **25**, 1745.
6 O. Sato, J. Tao, Y. Z. Zhang, *Angew Chem Int Ed*, 2007, **46**, 2152.
7 (a) L. Salmon, G. Molnar, D. Zitouni, C. Quintero, C. Bergaud, J.-C. Micheau, A. Bousseksou, *J. Mater. Chem* 2010, **20**, 5499;

(b) C. Bartual-Murgui, A. Akou, C. Thibault, G. Molnár, C. Vieu, L. Salmon, A. Bousseksou, *J. Mater. Chem. C* 2015, **3**, 1277.

8 (a)I. Suleimanov, O. Kraieva, G. Molnar, L. Salmon, A. Bousseksou, *Chem Commun* 2015, **51**, 15098; (b) S. Kume, K. Kuroiwa, N. Kimizuka, *Chem Commun* 2006, (23), 2442; (c) S. Cobo, G. Molnar, J. A. Real, A. Bousseksou, *Angew Chem Int Ed* 2006, **45**, 5786; *Angew Chem Int Ed* 2006, **118**, 5918; (d) G. Molnár, S. Cobo, J. A. Real, F. Carcenac, E. Daran, C. Vieu, A. Bousseksou, *Adv Mater* 2007, **19**, 2163; (e) S. Bonhommeau, G. Molnr, A. Galet, A. Zwick, J. A. Real, J. J. McGarvey, A. Bousseksou, *Angew Chem Int Ed* 2005, **117**, 4137; *Angew Chem Int Ed* 2005, **44**, 4069; (f) T. Forestier, S. Mornet, N. Daro, T. Nishihara, S. Mouri, K. Tanaka, O. Fouche, E. Freysz, J. F. Letard, *Chem Commun* 2008, 4327.

9 (a) P. Grondin, D. Siretanu, O. Roubeau, M. F. Achard, R. Clerac, *Inorg Chem* 2012, **51**, 5417; (b) M. M. Dirtu, A. Rotaru, A. Gillard, J. Linars, E. Codjovi, B. Tinant, Y. Garcia, *Inorg. Chem* 2009, **48**, 7838; (c) G. A. Ozin, A. C. Arsenault, Nanochemistry: A Chemical Approach to Nanomaterials, The Royal Society of Chemistry, Cambridge, 2005; (d) C. Burda, X. Chen, R. Narayanan, M.A. El-Sayed, *Chem. Rev* 2005, **105**, 1025; (e) A. Rotaru, I. A. Gural'skiy, G. Molnar, L. Salmon, P. Demont, A. Bousseksou, *Chem Commun* 2012, **48**, 4163; (f) M. B. Duriska, S. M. Neville, B. Moubaraki, J. D. Cashion, G. J. Halder, K. W. Chapman, C. Balde, J. F. Letard, K. S. Murray, C. J. Kepert and S. R. Batten, *Angew Chem Int Ed* 2009, **48**, 2549.

10 (a) F. Volatron, L. Catala, E. Riviere, A. Gloter, O. Stephan,T. Mallah, *Inorg. Chem* 2008, **47**, 6584; (b) O. Kahn, J. Krober, C. Jay *Adv. Mater*, 1992, **4**, 718; (c) Y. Raza, F. Volatron, S. Moldovan, O. Ersen, V. Huc, C. Martini, F. Brisset, A. Gloter, O. Stephan, A. Bousseksou, L. Catala, T. Mallah, *Chem Commun* 2011, **47**, 11501; (d) A. Lapresta-Fernández, M. P. Cuéllar, J. M. Herrera, A. Salinas-Castillo, M. d. C. Pegalajar, S. Titos-Padilla, E. Colacio, L. F. Capitán-Vallvey, *J. Mater. Chem. C*, 2014, **2**, 7292; (e) A. Lapresta-Fernandez, S. Titos-Padilla, J. M. Herrera, A. Salinas-Castillo, E. Colacio, L. F. Capitan Vallvey, *Chem Commun*, 2013, **49**, 288.

11 J. R. Galan-Mascaros, E. Coronado, A. Forment-Aliaga, M. Monrabal-Capilla, E. Pinilla-Cienfuegos, M. Ceolin, *Inorg Chem* 2010, **49**, 5706.

12 (a) T. Q. Hung, F. Terki, S. Kamara, M. Dehbaoui, S. Charar, B. Sinha, C. Kim, P. Gandit, I. A. Gural'skiy, G. Molnar, L. Salmon, H. J. Shepherd, A. Bousseksou, *Angew Chem Int Ed* 2013, **52**, 1185; (c) O. Roubeau, *Chemistry* 2012, **18**, 15230.

13 I. Boldog, A. B. Gaspar, V. Martinez, P. Pardo-Ibanez, V. Ksenofontov, A. Bhattacharjee, P. Gutlich, J. A. Real, *Angew Chem Int Ed* 2008, **47**, 6433.

14 Y. A. Tobon, C. Etrillard, O. Nguyen, J.-F. Létard, V. Faramarzi, J.-F. Dayen, B. Doudin, D. M. Bassani, F. Guillaume, *Eur. J. Inorg. Chem.* 2012, **2012**, 5837.

15 I. A. Gural'skiy, C. M. Quintero, G. Molnar, I. O. Fritsky, L. Salmon, A. Bousseksou, *Chemistry* 2012, **18**, 9946.

16 P. N. Martinho, T. Lemma, B. Gildea, G. Picardi, H. Muller-Bunz, R. J. Forster, T. E. Keyes, G. Redmond, G. G. Morgan, *Angew Chem Int Ed* 2012, **51**, 11995.

17 (a) A. Ceccon, M. Lelli, M. D'Onofrio, H. Molinari, M. Assfalg, *J Am Chem Soc* 2014, **136**, 13158; (b) M. L. Immordino, F. Dosio, L. Cattel, *Int. J. Nanomed* 2006, **1**, 297; (c) S. Bibi, E. Lattmann, A. R. Mohammed, Y. J. Perrie, *Microencapsulation* 2012, **29**, 262.

18 C. Bonnaud, C. A. Monnier, D. Demurtas, C. Jud, D. Vanhecke, X. Montet, R. Hovius, M. Lattuada, B. Rothen-Rutishauser, A. Petri-Fink. *ACS NANO* 2014, **8**, 3451.

19 (a) A. Nel, T. Xia, L. Mädler, N. Li, *Science* 2006, **311**, 622; (b) Y. Roiter, M. Ornatska, A. R. Rammohan, J. Balakrishnan, D. R. Heine, S. Minko, *Nano Lett* 2008, **8**, 941.

20 S. Kim, C. Bellouard, J. Eastoe, N. Canilho, S. E. Rogers, D. Ihiawakrim, O. Ersen, A. Pasc, *J Am Chem Soc* 2016, **138**, 2552.

21 (a) J. A. Real, M. C. Munoz, J. Faus, X. Solans, *Inorg. Chem* 1997, **36**, 3008; (b) A. Galet, A. B. Gaspar, G. Agusti, M. C. Muñoz, G. Levchenko, J. A. Real, *Eur. J. Inorg. Chem.* 2006, **2006**, 3571; (c) N. Moliner, L. Salmon, L. Capes, M. C. Munoz, J.-F. Letard, A. Bousseksou, J.-P. Tuchagues, J. J. McGarvey, A. C. Dennis, M. Castro, R. Burriel, J. A. Real, *J. Phys. Chem. B* 2002, **106**, 4276; (d) H. Naggert, A. Bannwarth, S. Chemnitz, T. von Hofe, E. Quandt, F. Tuczek, *Dalton Trans* 2011, **40**, 6364; (e) A. Pronschinske, R. C. Bruce, G. Lewis, Y. Chen, A. Calzolari, M. Buongiorno-Nardelli, D. A. Shultz, W. You, D. B. Dougherty, *Chem Commun* 2013, **49**, 10446.

22 Y.-H. Luo, M. Nihei, G.-J. Wen, B.-W. Sun, H. *Inorg. Chem.* 2016, DOI: 10.1021/acs.inorgchem.6b01193.

23 (a) H. Soyer, E. Dupart, C.J. Garlos-Garcia, C. Mingotaud, P. Delhaes, *Adv. Mater* 1999, **11**, 382; (b) S. MaterHayami, K. Danjobara, K. Inoue, *Adv. Mater* 2004, **16**, 869; (c) H, Matsukizono, K. Kuroiwa, N. Kimizuka, *J. Am. Chem. Soc*. 2008, **130**, 5622.

24 (a) H. B. Duan, X. M. Ren, L. J. Shen, W. Q. Jin, Q. J. Meng, Z. F. Tian, S. M. Zhou, *Dalton Trans* 2011, **40**, 3622; (b) S. Hayami, M. R. Karim,Y. H. Lee, *Eur. J. Inorg. Chem.* 2013, **2013**, 683; (c) M. Seredyuk, A. B. Gaspar, V. Ksenofontov, Y. Galyametdinov, J. Kusz, P. Gütlich, *Adv. Func. Mater.* 2008, **18**, 2089; (d) M. Seredyuk, A. B. Gaspar, V. Ksenofontov, Y. Galyametdinov, M. Verdaguer, F. Villain, P. Gutlich, *Inorg Chem* 2010, **49**, 10022.

25 (a) T. Fujigaya, D. L. Jiang, T. Aida, *Chem Asian J* 2007, **2**, 106; (b) O. Roubeau, A. Colin, V. Schmitt, R. Clerac, *Angew Chem Int Ed* 2004, **43**, 3283.

26 (a) J. Sniekers, K. Verguts, N. R. Brooks, S. Schaltin, T. H. Phan, T. M. Trung Huynh, L. Van Meervelt, S. De Feyter, J. W. Seo, J. Fransaer, K. Binnemans, *Chemistry*, 2016, **22**, 1010; (b) M. Gerigk, P. Ehrenreich, M. R. Wagner, I. Wimmer, J. S. Reparaz, C. M. Torres, L. Schmidt-Mende, S. Polarz, *Nanoscale*, 2015, **7**, 16969.

27 M. S. Vickers, K. S. Martindale, P. D. Beer, *J. Mater. Chem*, 2005, **15**, 2784.

28 (a) M. Nihei, Y. Suzuki, N. Kimura, Y. Kera, H. Oshio, *Chemistry* 2013, **19**, 6946; (b) Y. H. Luo, L. J. Yang, Q. L. Liu, Y. Ling, W. Wang, B. W. Sun, *Dalton Trans* 2014, **43**, 16937.

29 S. Fang, Y. Niu, W. Zhu, Y. Zhang, L. Yu, X. Li, *Chem Asian J* 2015, **10**, 1232.

30 D. Pucci, G. Barberio, A. Crispini, M. Ghedini, O. Francescangeli, *Molecular Crystals and Liquid Crystals*, 2003, **395**, 325.

31 (a) M. S. Vickers, K. S. Martindale, P. D. Beer, *J. Mater. Chem.* 2005, **15**, 2784; (b) J. D. Blakemore, A. Gupta, J. J. Warren, B. S. Brunschwig, H. B. Gray, *J. Am. Chem. Soc.* 2013, **135**, 18288.

32 R. Kulmaczewski, H. J. Shepherd, O. Cespedes, M. A. Halcrow, *Inorg. Chem.* 2014, **53**, 9809.

33 Rigaku, CrystalClear, Version 14.0. Rigaku Corporation, Tokyo, Japan, 2005.

34 M. Sheldrick, SHELXS97: Programs for Crystal Structure Analysis, University of Gottingen, Germany, 1997.

35 Mercury 2.3 Supplied with Cambridge Structural Database, CCDC: Cambridge, UK, 2003-2004.

View Article Online
DOI: 10.1039/C6TC02796B



Table of contents

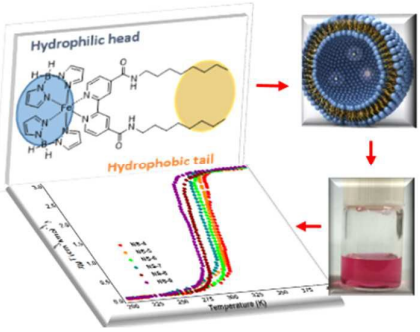


Above room-temperature spin-transition have been achieved in a series vesicular nano-sphere, which were prepared via liposomal self-assembly strategy.